High Resolution Measurements of Ion Upflow and Downflow Within the Northern Polar Cusp

N. H. Godbole[1], M. R. Lessard[1], B. Fritz[1,2], D. Kenward[1], K. A. Lynch[3], M. Harrington[3], T. M. Roberts[3], P. A. Fernandes[3,4], M. Zettergren[5], J. Clemmons[1,6], J. Hecht[6], D. Hysell[7], K. Oksavik[8], J. Moen[9], L. Clausen[9] , F. Sigernes[10], T. Yeoman[11]

Space Sciences Center, University of New Hampshire[1], Naval Research Laboratory[2], Department of Physics and Astronomy, Dartmouth College[3], ISR-1 Space Science and Applications, Los Alamos National Laboratory[4], Physical Sciences Department, Embry-Riddle Aeronautical University[5], Aerospace Corporation[6], Department of Earth and Atmospheric Sciences, Cornell University[7], Department of Physics and Technology, University of Bergen[8], Department of Physics, University of Oslo[9], UNIS Aurora Observatory and Kjell Henriksen Observatory (KHO)[10], Department of Physics and Astronomy, University of Leicester[11]

University of New Hampshire

Abstract

We present an analysis of in-situ thermal ion measurements made by the Rocket Experiment for Neutral Upwelling (RENU2) sounding rocket by comparing observational data with modeled results to create a database of most-probable ambient ion temperature (parallel and perpendicular), anisotropy, and parallel flow. RENU2 was launched on December 13, 2015 from the Andøya Space Center (Norway) into a neutral upwelling event to study particle behavior between 200 km and 450 km. RENU2 provides an unprecedentedly complete picture of the auroral particle environment in a dayside cusp event, including charged particle observations from thermal electrons and ions, and precipitating energetic electrons and ions. RENU2 utilizes Hemispherical Energy Particle Spectrometers (HEEPS-M, HEEPS-T, and BEEPS-T) electrostatic analyzers, spanning a range from 0.122 eV to 791 eV, to investigate the relationship between ion outflow and neutral upwelling. These instruments measure two-dimensional ion distribution functions from the spinning field-aligned main payload, providing information regarding temperature enhancement, bulk flow, anisotropy and conics. By modeling Maxwellian distributions constrained by other diagnostics (eg. GPS velocity, DC electric field, radar density profiles, ambient electron temperature for the sheath potential) that best fit the data and comparing to the observed distribution slices, we are able to establish a database of most-probable thermal ion temperature, anisotropy, and parallel flow over the course and duration of RENU2's flight. This process has thus far confirmed observations of ion upflow (t = 575 s) within the cusp precipitation and downflow (t = 346 s) equatorward of the precipitation boundary during the course of the flight, and reproduced the expected jumps in temperature corresponding to the rocket's entering an auroral arc at t = 450 s. The measurements derived from minimizing the difference between real observations and constrained modeled results will be used as inputs for coupled ionospheric system models.

Introduction

Understanding the evolution of magnetospheric dynamics provides insight into planetary atmospheres. One aspect of this involves the net loss of atmospheric particles to space through a process called planetary escape, in which ions are accelerated to velocities sufficient to escape Earth's gravitational field. Ion Outflow is the process through which ions achieve energies sufficient for planetary escape. This net acceleration is achieved via a two-step process, illustrated by Figure 1.

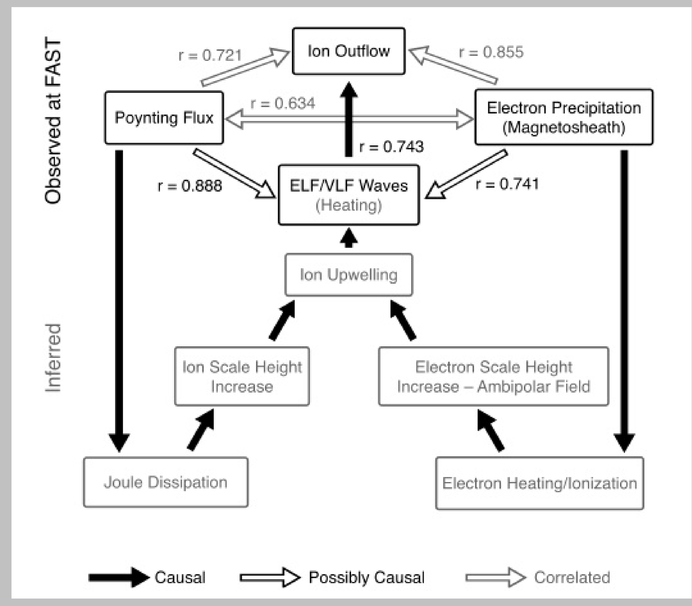

Figure 1: Flow chart relating factors contributing to ion outflow. [Strangeway et al. , 2004]

The first step in this process is called Ion Upflow, in which ions are accelerated but do not achieve escape velocity. Upflow can result from two distinct processes: Type I (Joule heating), and Type II (electron precipitation) respectively.

In the second step, Ion Outflow, additional energization processes must occur to accelerate ions to escape velocity. This usually occurs through wave-particle interactions (WPIs). Without these higher-altitude interactions, upflowing ions will eventually return to their lower altitudes, producing net downflow. At the low altitudes of ionospheric sounding rockets (several hundred km), the downflow signature can be prevalent; this is seen both as a downflowing vertex of energetic ion conics [Arnoldy et al. , 1996], and as an overall downflow of the bulk thermal ion population as shown here.

Instrumentation

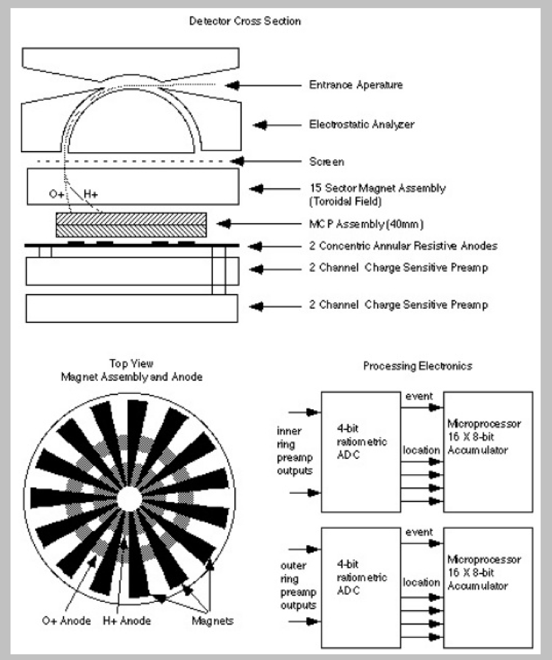

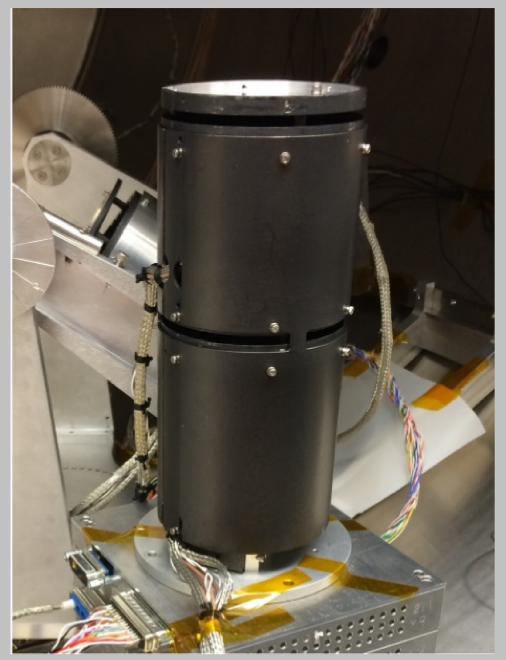

Figure 2: (left) Schematic displaying a cross section of the BEEPS ESA. HEEPS shares this design, excluding the toroidal magnetic field. [M. Witholm (UNH) in Harrington , 2016] (right) Photo of the integrated detector stacked in the can assembly prior to its installation on the main payload. The exterior can is coated with a layer of Aerodag to allow a smooth equipotential outer surface; the interior electrostatic surfaces are coated with copper black to reduce UV scatter. [Harrington , 2016]

Flight Overview

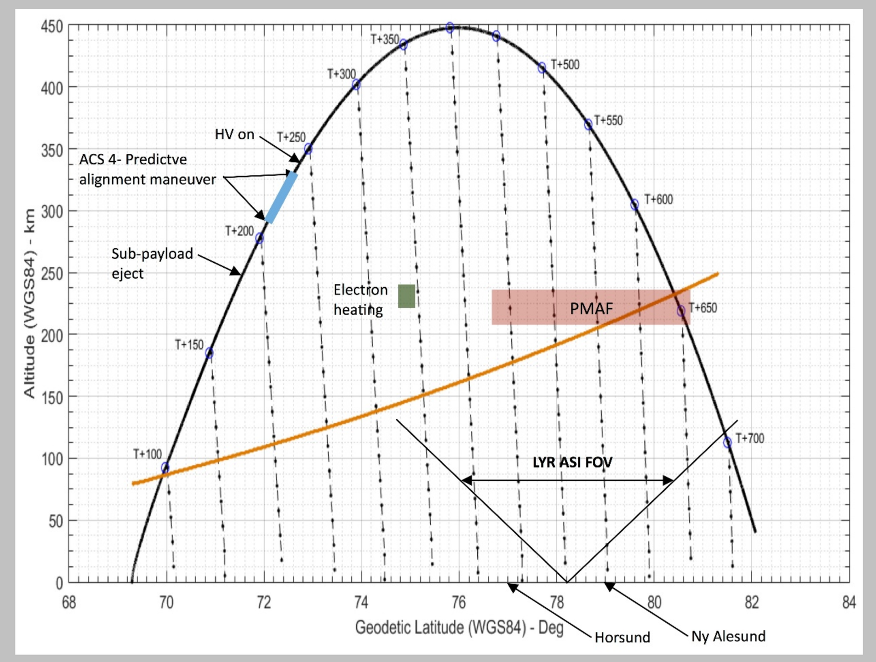

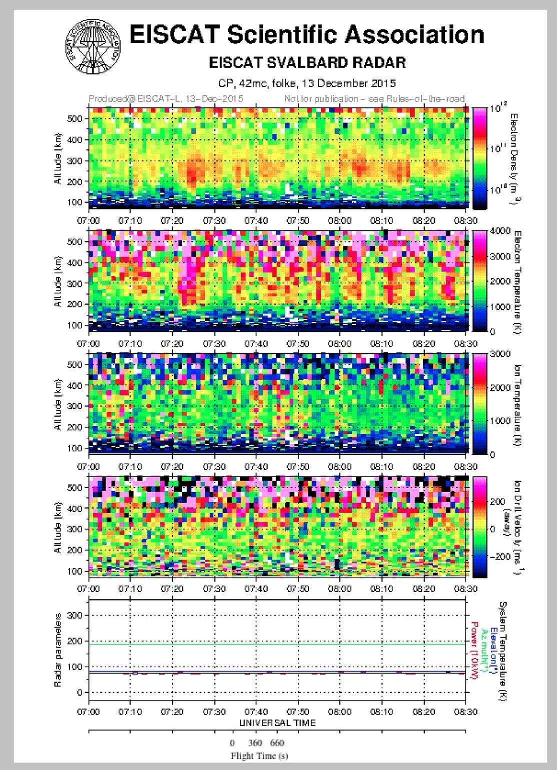

Figure 3: (left) Flight trajectory of RENU2. The orange line denotes the shadow, while the PMAF region is denoted in red. RENU2 entered the auroral arc at approximately t = 450 s. [Lessard , 2016] (right) Electron data from the EISCAT Svalbard radar indicates multiple transients in temperature, consistent with PMAF activity. Further, weak ion upflow can be seen above 400 km throughout the interval. Between 07:34 and 07:48 UT, upflow has extended down to 300 km. [Oksavik , 2016]

Maxwellian Fits

High collision rates among particles at rocket altitudes foster thermal equilibrium. Thus, the thermal ion population can be modeled using a Maxwellian distribution, assuming isotropic temperature conditions (and bi-Maxwellian for an anisotropic temperature). [Fernandes , 2016]

HEEPS-T allows us to measure 2D ion distributions, BUT, we don't necessarily know the input values that produce such a distribution. Hence, fitting is required to characterize in-situ ion temperatures and velocities.

In a nutshell, we:

- constrain known parameters including relative plasma motion (from DCE and GPS data), payload potential (from electron temperature data), and density (from an altitude and activity dependent proxy based on nearby EISCAT data).
- allow a range of possible values for the ion temperature and parallel bulk flow velocity.
- generate Maxwellian distributions using each permutation therein, and slice them consistent with the attitude of the detector aperture at each time step.
- minimize the difference (as a function of ion temperature and parallel velocity choices) between the Maxwellian slice, and the actual data for each time slice record the corresponding output ion temperature and parallel bulk velocity values.

Results

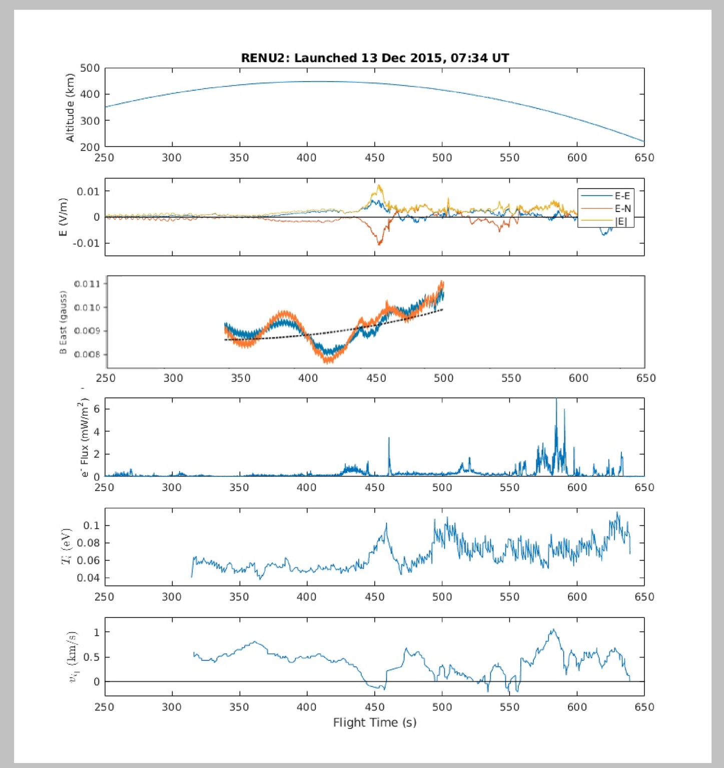

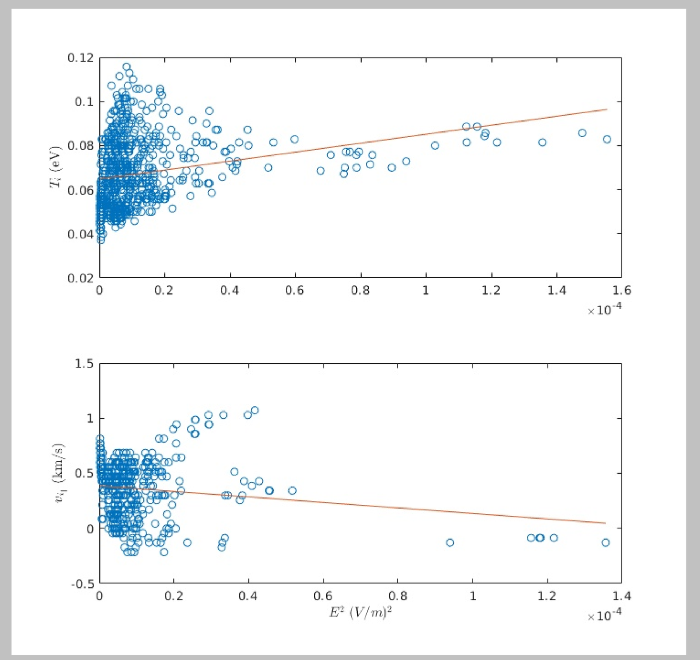

Figure 4: (left) Comparison of fitted results to measured data. From top to bottom: payload altitude, electric and magnetic field components and magnitude, electron flux (from EPLAS instrument), best-fit ion temperature, and best-fit parallel velocity vs. flight time. The best-fit parameters have been filtered using a seven-point moving average filter. The parallel velocity characterizes the degree of upflow (negative) and downflow (positive) present along the local magnetic field. The velocity data suggests the presence of a cold, downflowing filament between 535 and 545s, followed by a warm, upflowing filament between 545 and 555s. There is not a local relationship to the concurrent PMAF electron flux data, since the timescales of electron precipitation and ion heating are very different. It is interesting to note the narrow confinement of the heated ion structures. (see Figure 5)
(right) Scatter-plots of the best-fit ion temperature (top) and best-fit parallel velocity (bottom) against the magnitude of the electric field squared. The orange lines denote the least-squares regression fit to the data. The ion temperature and the local DCE are related through expectations of collisional drag (see Figure 6)

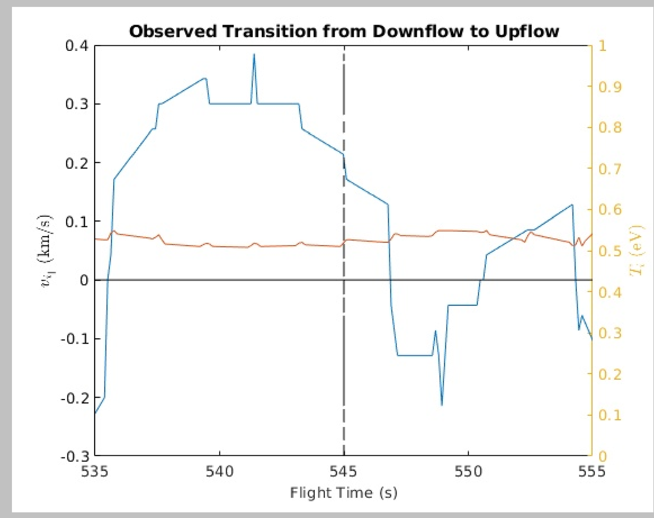

Figure 5: Close-up of the parallel velocity and ion temperature vs. flight time displaying the transition from a cold, downflowing filament (535 to 545s), to a warm, upflowing filament (545 to 550s), followed by another downflowing filament (550 to 555s). The first filament is approximately 20km over 10s, with subsequent events 10km in extent, over 5s (payload velocity 2km/s in this region). The observed transitions occur over approximately 5km.

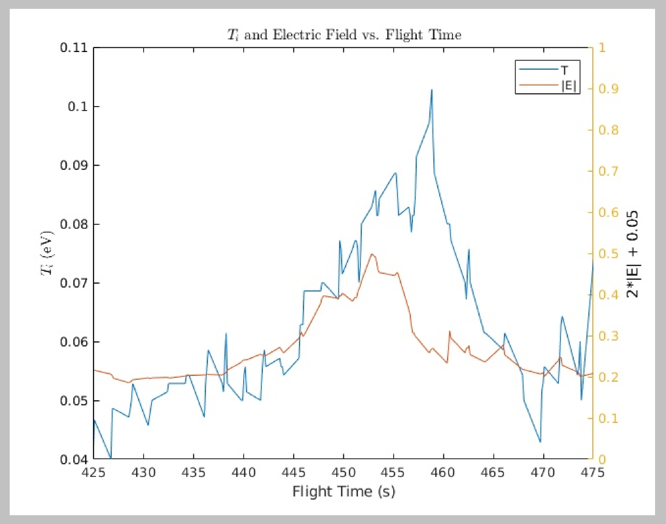

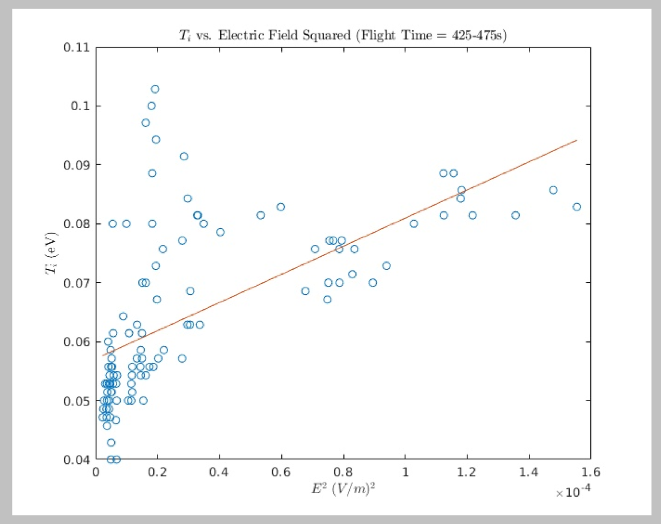

Figure 5: (left) Close-up of the ion temperature and electric field magnitude vs. flight time, displaying the strong correlation of electric field and ion temperature between 425 and 475s. (right) Scatter plot of T_i vs E^2 for this time interval. The relationship is much clearer here than elsewhere in the flight, most likely because this comparison ignores the neutral wind effects (see below.)

The relationship between ion temperature and electric field is given by:

$$T_i = T_n + 37.5(\vec{E} + \vec{u_n} \times \vec{B})$$

...where T_i and T_n are the ion and neutral temperatures respectively, E and B are the electric and magnetic fields, and u_n are the neutral velocities. [Schunk and Nagy , 2009 ; Fernandes , 2016]

The neutral wind velocities along RENU2's trajectory are on the order of km/s, an order of magnitude larger than the ExB velocity from the small local DCE. The observed lack of clear correlation during the majority of the flight could result from the neutral winds dominating the electric field contribution to the ion temperature. The scatterplot on the right, here limited to T + 425s to 475s, ignores the u_n term of the expected relationship. The orange line denotes the least-squares regression fit to the data. The y-intercept provides an estimate for the neutral temperature. Here, it is approximately 0.06eV.

Summary

- Quantifying the degree of spatial and/or temporal variance of filamentary structures in the ionosphere provides insight into the shared vs. unshared histories of constituent particle groups. Specifically, it is implied that downflowing populations have shared history, in that they must have first achieved upflow before being able to return to lower altitudes. Such downflowing filamentary structures were originally noted by Arnoldy et al. , 1996.
- Figure 5 provides an example of three adjacent downflowing and subsequent upflowing filaments. The largest is approximately 20km over 10s, with subsequent events of order 10km in extent, over 5s, with transitions of order 5 km. We would like to better understand the differences between these spatial and temporal scales in how they impact the evolution of filamentary structures.
- We would like to gain a better understanding of the factors controlling the ion temperature. To this end, the next step in our analysis involves incorporating the neutral wind magnitude and directional data from J. Clemmons into Figure 6.

References

Arnoldy, R. L., K. A. Lynch, P. M. Kintner, J. W. Bonnell, T. E. Moore, and C. J. Pollock (1996), SCIFER—Structure of the cleft ion fountain at 1400 km altitude, Geophys. Res. Lett., 23(14), 1869–1872.

Burchill, J. K., et al. (2010), Thermal ion upflow in the cusp ionosphere and its dependence on soft electron energy flux, J. Geophys. Res., 115, A05206, doi:10.1029/2009JA015006.

Cohen, I. J., et al. (2016), Rocket-borne measurements of electron temperature and density with the Electron Retarding Potential Analyzer instrument, J. Geophys. Res. Space Physics, 121, 67746782

Fernandes, P. A., et al. (2016), Measuring the seeds of ion outflow: Auroral sounding rocket observations of low-altitude ion heating and circulation, J. Geophys. Res. Space Physics, 121, 1587–1607, doi:10.1002/2015JA021536.

Harrington, M. (2017), RENU2 Sounding Rocket Analysis: Ion Database Construction, Master of Science in Physics and Astronomy, Dartmouth College, Hanover, NH

Schunk, R. W., and A. Nagy (2009), Ionospheres: Physics, Plasma Physics, and Chemistry, 2nd ed., Cambridge Univ. Press, Cambridge, U. K.

Strangeway, R. J., et al. (2005), Factors controlling ionospheric outflows as observed at intermediate altitudes, J. Geophys. Res., 110, A03221

contact: nhg1005@wildcats.unh.edu